Supplemental Information

An UNC13A^{P814L}-variant causes increased synaptic transmission and dyskinetic movement disorder

Noa Lipstein,[1] Nanda M. Verhoeven-Duif,[2,3] Francesco E. Michelassi,[4] Nathaniel Calloway,[4] Peter M. van Hasselt,[5] Katarzyna Pienkowska,[1] Gijs van Haaften,[2,3] Mieke M. van Haelst,[3] Ron van Empelen,[6] Inge Cuppen,[7] Heleen C. van Teeseling,[8] Annemieke M.V. Evelein,[9] Jacob A, Vorstman,[9] Sven Thoms,[10] Olaf Jahn,[11] Karen J. Duran,[2,3] Glen R. Monroe,[2,3] Timothy A. Ryan,[4] Holger Taschenberger,[1] Jeremy S. Dittman,[4] Jeong-Seop Rhee,[1], Gepke Visser,[5] Judith J. Jans,[3,*] and Nils Brose[1,*]

[1]Department of Molecular Neurobiology, Max Planck Institute of Experimental Medicine, Göttingen, Germany.

[2]Center for Molecular Medicine, University Medical Center Utrecht, Utrecht, The Netherlands.

[3]Department of Genetics, University Medical Center Utrecht, Utrecht, The Netherlands.

[4]Department of Biochemistry, Weill Cornell Medical College, New York, NY, USA.

[5]Department of Pediatric Metabolic Diseases, Wilhelmina Children's Hospital, Utrecht, The Netherlands.

[6]Child Development and Exercise Center, Division of Paediatrics, University Medical Center Utrecht, Utrecht, The Netherlands.

[7]Department of Paediatric Neurology, Wilhelmina Children's Hospital, University Medical Center Utrecht, Utrecht, The Netherlands.

[8]Department of Paediatric Psychology, Sector of Neuropsychology, University Medical Center Utrecht, Utrecht, The Netherlands.

[9]Brain Center Rudolf Magnus, Department of Psychiatry, University Medical Center Utrecht, Utrecht, The Netherlands.

[10]Department of Pediatrics and Pediatric Neurology, University Medical Center, Georg August University, Göttingen, Germany.

[11]Proteomics Group, Max Planck Institute of Experimental Medicine, Göttingen, Germany.

Content

1. Additional Clinical Information

2. Supplemental Video Legends

3. Supplemental Figure 1

4. Supplemental Figure 2

5. Supplemental Figure 3

6. Supplemental Bibliography

Additional clinical information and psychiatric evaluation. Prior to whole exome sequencing, the patient underwent genetic screening (Angelman syndrome and Fragile-X) and extended metabolic screening of urine, plasma, and cerebrospinal fluid. No obvious aberrant metabolites were detected. In March 2014, at the age of 4 years and 10 months, the patient was evaluated in the Outpatient Clinic of the Department of Child and Adolescent Psychiatry at the University Medical Center Utrecht. Psychiatric evaluation of the boy was performed by a registered child and adolescent psychiatrist (JAV). In addition to a systematic screening of possible psychiatric disorders following the DSM-IV criteria, the Autism Diagnostic Observation Schedule 2 (ADOS-2) module 2 and the Autism Diagnostic Interview Revised (ADI-R) were used by a trained psychologist to assess the possibility of a disorder in the autistic spectrum. The parents described their son as a cheerful boy, even though he often lacks social responsiveness, often misses social cues, and shows socially inappropriate behaviors. In addition, he strongly holds on to daily routines and to the ordering of his room. Only recently, he has started to engage in limited functional play such as rolling toy cars. His parents noted a tendency to eat inedible things (pica). He is also described as very impulsive and hyperactive. At the child day care center, similar symptoms were observed. He shows excessive perseverance and several repetitive behaviors, and has difficulties in reciprocal playing with other children. His concentration span is limited in comparison to his peers. The psychiatric family history was negative for ASD, attention deficit and hyperactivity disorder (ADHD), and other psychiatric disorders. At the time of evaluation, the patient did not use any medication. During psychiatric examination, the boy showed behaviors consistent with autism. Based on the clinical evaluation and the additional diagnostic tests, including the ADOS-2 and the ADI-R, the diagnosis of autistic disorder was made. In December 2015 a second assessment was performed (by the same psychiatrist) during which the previous observations indicative of autism were confirmed.

In addition, his ADHD behaviors persevered despite the adaptation to an environment that was better adjusted to his competencies and needs. Therefore, an additional diagnosis of ADHD was now deemed appropriate.

Limitations of psychiatric assessment. Although the DSM-IV provides criteria for a wide range of diagnostic classifications, the individual psychiatric phenotype can manifest in many combinations of behavior, not always consistent with one particular diagnostic label. With regard to the psychiatric phenotype of the case presented here, the diagnosis ASD could be made at the time of evaluation. Although the boy also showed hyperactivity, concentration problems, and impulsivity, ADHD was initially not diagnosed since these symptoms could also be explained by, at that time, suboptimal adaptation of the home and school environment to the needs of the patient. However, at the second assessment, sufficient criteria were met to justify a separate, co-morbid diagnosis of ADHD. Further follow-up of the child will be informative with respect to developmental changes in characteristics of the phenotype.

Supplemental Video Legends

The video shows the patient at the age of 2 years. The first part demonstrates his restlessness and continuous moving pattern. In the second part, choreoathetosis and tremor can be observed.

Supplemental Figure 1

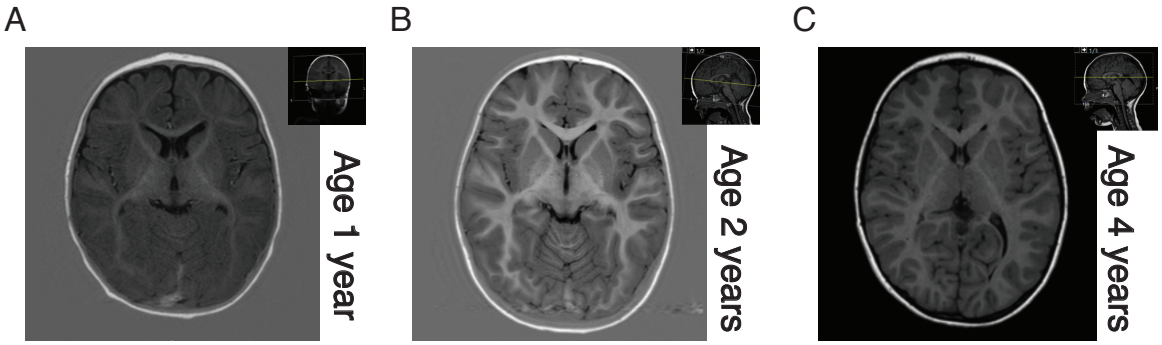

Figure S1. T1 weighted brain MRI images at the basal ganglia at age 1 year (**A**), 2 years (**B**) and 4 years (**C**). No structural abnormalities, signs of leukodystrophy or abnormalities are seen.

Supplemental Figure 2

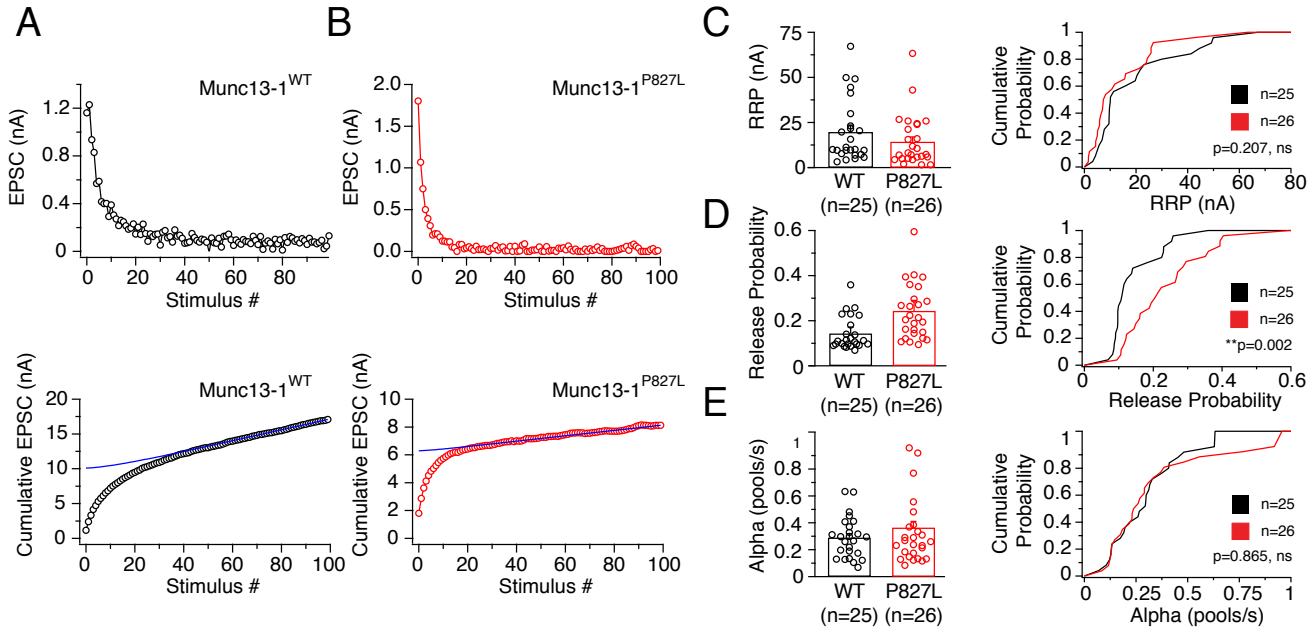

Figure S2. Detailed analysis of synaptic depression during 40 Hz trains provides estimates for pool size (RRP), release probability (P), and SV replenishment rate (α). (**A**, **B**) Representative plots of EPSC amplitudes recorded in Munc13-1/2 DKO autaptic neurons expressing Munc13-1^{WT} (**A**, black) or Munc13-1^{P827L} (**B**, red) in response to a 40 Hz train consisting of 100 stimuli. Bath solution contained 4 mM Ca^{2+} and 4 mM Mg^{2+}. The cumulative EPSC amplitudes are plotted in the bottom panels. Since the 40 Hz train leads to near depletion, the blue lines in the bottom panels represent estimates for the sum of SVs that were (i) present in the RRP before the train and (ii) those that were newly recruited to the RRP, assuming the 1st order kinetics of the replenishment process. Analysis was performed following Wessling and Lo (1), assuming a simple kinetic scheme of a single SV pool that is consumed with a unitary rate of exocytosis and replenished with a fixed replenishment rate constant alpha. (**C**) Left: A plot depicting the predicted RRP size (in nA). Individual values per neuron are indicated as circles (Munc13-1^{WT}, black, 19.7 ± 3.9 nA, n=25 vs. Munc13-1^{P827L}, red, 14.2 ± 2.7 nA, n=26). Right: Cumulative probability distribution of the values shown in the left panel (p>0.05; Kolmogorov-Smirnov test). (**D**) Left: A plot depicting the predicted release probability (P). Individual values per neuron are indicated as circles (Munc13-1^{WT}, black, 0.143 ± 0.029, n=25 vs. Munc13-1^{P827L}, red, 0.243 ± 0.047 nA, n=26). Right: Cumulative probability distribution of the values shown in the left panel (p<0.01; Kolmogorov-Smirnov test). Note the right-shift of the cumulative probability distribution of P obtained from Munc13-1^{P827L} autapses, resulting in an increase of the mean P value by ~70%. (**E**) Left: A plot depicting the predicted replenishment rate constant (alpha). Individual values per neuron are indicated as circles (Munc13-1^{WT}, black, 0.289 ± 0.058 pools/s, n=25 vs. Munc13-1^{P827L}, red, 0.364 ± 0.070 pools/s, n=26). Right: Cumulative probability distribution of the values shown in the left panel (p>0.05; Kolmogorov-Smirnov test). All error bars represent mean±SEM.

Supplemental Figure 3

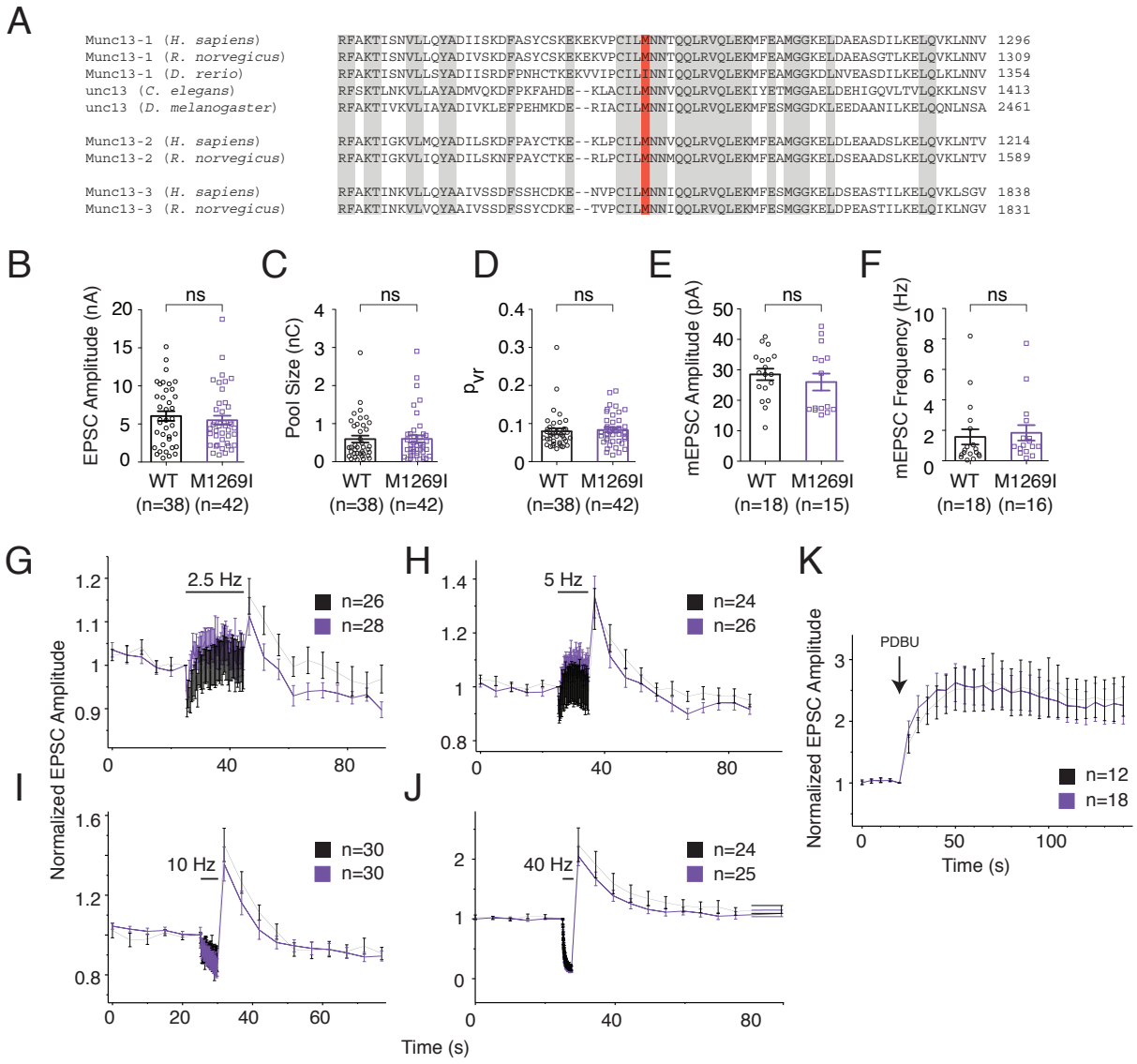

Figure S3. Synaptic transmission characteristics of autaptic neurons expressing Munc13-1^{M1269I}. **(A)** Amino acid alignment of Munc13 proteins from the indicated organisms showing sequence identity (grey) in the region covering the mutated Methionine (red). Autaptic hippocampal neurons were prepared from Munc13-1/Munc13-2 DKO mouse brains and were infected with a lentivirus to mediate the expression of Munc13-1^{WT} (black) or Munc13-1^{M1269I} (purple). The neurons were whole-cell voltage clamped and synaptic transmission was assessed. **(B)** Average initial EPSCs in neurons expressing Munc13-1^{WT} or Munc13-1^{M1269I}. Individual average values per neuron are indicated as circles ($p>0.05$; Mann-Whitney test). (**C**) RRP size estimated by application of 0.5 M sucrose. Individual values per neuron are indicated as circles ($p>0.05$; Mann-Whitney test). (**D**) Release probability (P_{vr}) calculated by dividing the charge transfer during the EPSC by the charge transfer during the sucrose application. Individual values per neuron are indicated as circles ($p>0.05$; Mann-Whitney test). (**E,F**) mEPSC amplitudes (**E**) and mEPSC frequency (**F**). Individual values per neuron are indicated as circles

(p>0.05; Mann-Whitney test). (**G**-**J**) Neurons were stimulated with AP trains at frequencies of 2.5 Hz (**G**), 5 Hz (**H**), 10 Hz (**I**), and 40 Hz (**J**), flanked by ongoing 0.2 Hz stimulation. Amplitudes were normalized to the average amplitude before the train. (**K**) Potentiation of the EPSC in response to a 2 min application of 1 μM PDBu (start of application is labeled by an arrow). The neurons were stimulated at 0.2 Hz. Error bars in (**B-K**) represent mean±SEM. ns, p>0.05.

Supplemental Bibliography

1. Wesseling JF, and Lo DC. Limit on the role of activity in controlling the release-ready supply of synaptic vesicles. *J Neurosci.* 2002;22(22):9708-9720.